NASA/TM—2001-211135 AIAA–2001–3774

High Voltage SPT Performance

David Manzella
University of Toledo, Toledo, Ohio

David Jacobson and Robert Jankovsky
Glenn Research Center, Cleveland, Ohio

November 2001

The NASA STI Program Office . . . in Profile

Since its founding, NASA has been dedicated to the advancement of aeronautics and space science. The NASA Scientific and Technical Information (STI) Program Office plays a key part in helping NASA maintain this important role.

The NASA STI Program Office is operated by Langley Research Center, the Lead Center for NASA's scientific and technical information. The NASA STI Program Office provides access to the NASA STI Database, the largest collection of aeronautical and space science STI in the world. The Program Office is also NASA's institutional mechanism for disseminating the results of its research and development activities. These results are published by NASA in the NASA STI Report Series, which includes the following report types:

- TECHNICAL PUBLICATION. Reports of completed research or a major significant phase of research that present the results of NASA programs and include extensive data or theoretical analysis. Includes compilations of significant scientific and technical data and information deemed to be of continuing reference value. NASA's counterpart of peer-reviewed formal professional papers but has less stringent limitations on manuscript length and extent of graphic presentations.

- TECHNICAL MEMORANDUM. Scientific and technical findings that are preliminary or of specialized interest, e.g., quick release reports, working papers, and bibliographies that contain minimal annotation. Does not contain extensive analysis.

- CONTRACTOR REPORT. Scientific and technical findings by NASA-sponsored contractors and grantees.

- CONFERENCE PUBLICATION. Collected papers from scientific and technical conferences, symposia, seminars, or other meetings sponsored or cosponsored by NASA.

- SPECIAL PUBLICATION. Scientific, technical, or historical information from NASA programs, projects, and missions, often concerned with subjects having substantial public interest.

- TECHNICAL TRANSLATION. English-language translations of foreign scientific and technical material pertinent to NASA's mission.

Specialized services that complement the STI Program Office's diverse offerings include creating custom thesauri, building customized data bases, organizing and publishing research results . . . even providing videos.

For more information about the NASA STI Program Office, see the following:

- Access the NASA STI Program Home Page at *http://www.sti.nasa.gov*

- E-mail your question via the Internet to help@sti.nasa.gov

- Fax your question to the NASA Access Help Desk at 301–621–0134

- Telephone the NASA Access Help Desk at 301–621–0390

- Write to:
  NASA Access Help Desk
  NASA Center for AeroSpace Information
  7121 Standard Drive
  Hanover, MD 21076

NASA/TM—2001-211135 AIAA–2001–3774

High Voltage SPT Performance

David Manzella
University of Toledo, Toledo, Ohio

David Jacobson and Robert Jankovsky
Glenn Research Center, Cleveland, Ohio

Prepared for the
37th Joint Propulsion Conference and Exhibit
cosponsored by the AIAA, SAE, AIChE, and ASME
Salt Lake City, Utah, July 8–11, 2001

National Aeronautics and
Space Administration

Glenn Research Center

November 2001

Available from

NASA Center for Aerospace Information
7121 Standard Drive
Hanover, MD 21076

National Technical Information Service
5285 Port Royal Road
Springfield, VA 22100

Available electronically at http://gltrs.grc.nasa.gov/GLTRS

HIGH VOLTAGE SPT PERFORMANCE

David Manzella
University of Toledo
Toledo, Ohio 43606

David Jacobson and Robert Jankovsky
National Aeronautics and Space Administration
Glenn Research Center
Cleveland, Ohio 44135

SUMMARY

A 2.3 kW stationary plasma thruster designed to operate at high voltage was tested at discharge voltages between 300 and 1250 V. Discharge specific impulses between 1600 and 3700 sec were demonstrated with thrust between 40 and 145 mN. Test data indicated that discharge voltage can be optimized for maximum discharge efficiency. The optimum discharge voltage was between 500 and 700 V for the various anode mass flow rates considered. The effect of operating voltage on optimal magnet field strength was investigated. The effect of cathode flow rate on thruster efficiency was considered for an 800 V discharge.

INTRODUCTION

Over the last several decades research and development of Hall thruster propulsion has focused on a number of technical objectives. These include: the qualification of Hall thruster systems for on-orbit station keeping with powers ranging from near 1 kW up to 5 kW (refs. 1 to 3), the development of Hall thrusters and systems that operate efficiently at the specific impulses suitable for station-keeping and can also provide a high thrust-to-power ratio for orbit insertion of low Earth orbit (LEO) and geosynchronous orbit (GEO) spacecraft (refs. 4 and 5), the investigation of low power Hall thrusters for use on small, power limited spacecraft (ref. 6), and investigations into high power Hall thrusters for a new class of missions including LEO to GEO space transportation, human exploration and development of space (HEDS) (refs. 7 and 8), and space solar power. This investigation considers Hall thrusters capable of operation at specific impulses above the current state-of-the-art (1500 to 1800 sec), but less than that provided by state-of-the-art gridded ion thruster systems (3000 sec and above).

The motivation for this investigation is that propulsion systems utilizing Hall thrusters with specific impulses between 1800 and 3000 sec may offer substantial spacecraft mission benefits (ref. 9). These may include either a reduction in spacecraft wet mass (often times permitting a reduction in launch vehicle class) or an increase in spacecraft lifetime (at the expense of longer trip time or firing duration for power limited applications). However, measurements of the operational characteristics of Hall thrusters operating in this range of specific impulse are required to more accurately estimate these potential benefits.

To that end, NASA Glenn Research Center (GRC) solicited proposals for thrusters with performance characteristics approaching those of the state-of-art NSTAR gridded ion thruster. The specific goal was to obtain 2.3 kW laboratory model thrusters that could operate using xenon as the propellant at 3200 sec while providing 100 mN of thrust. Two suppliers were selected to build such thrusters. The first supplier was the Boeing Corporation that proposed a two stage anode layer thruster (TAL). Jacobson, et al., (ref. 10) provides details regarding the characteristics of this thruster in a companion paper. The second supplier selected was Atlantic Research Corporation (ARC). The thruster they supplied, which was fabricated through subcontract to the Fakel Design Bureau in Russia, is a stationary plasma thruster (SPT) of hybrid design. This design utilized a conventional dielectric material for the discharge chamber near the thruster exit plane and used metal construction as in TAL thrusters for the rear of the discharge chamber. The following report will summarize the important characteristics of this thruster, indicate the test apparatus used for and experimental evaluation of the thruster at GRC, and discuss the significance of these results.

APPARATUS AND PROCEDURE

The hybrid SPT thruster provided by ARC is a design derived from the flight model SPT–100 thruster. A photograph of this thruster, called the SPT–1, is shown in figure 1. The nominal outside diameter of the discharge chamber was 100 mm. While it was possible to independently supply propellant at the rear or either side of the annular anode, all testing was conducted with 100 percent of the xenon anode flow injected at the rear. The thruster

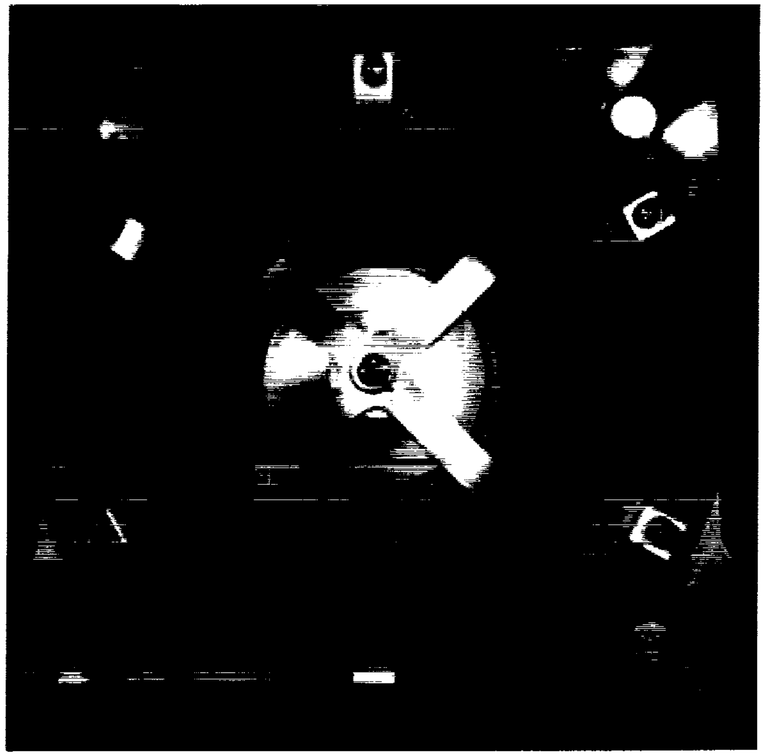

Figure 1.—SPT-1 high voltage stationary plasma thruster.

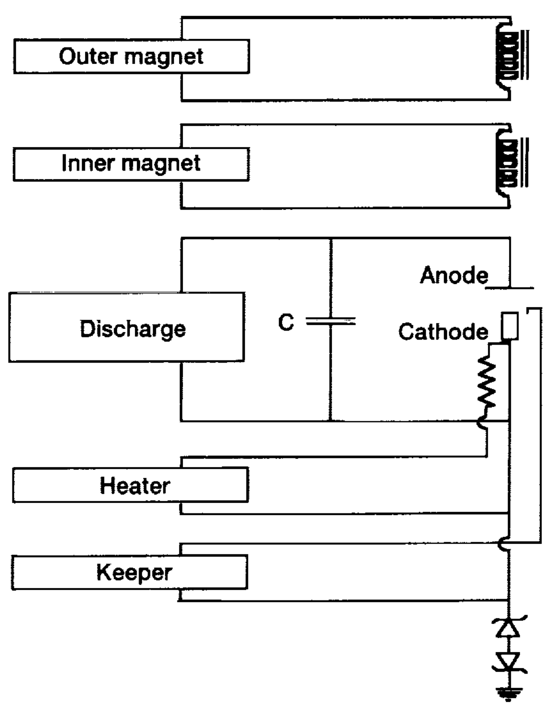

Figure 2.—Electrical schematic of test configuration.

was operated at total input powers between 1.0 and 3.2 kW. This was accomplished by providing anode xenon flow rates ranging from 2.4 to 5.4 mg/sec at discharge voltages between 300 and 1250 V. A laboratory model cathode was used for all testing. Neither cathode position nor cathode flow rate was optimized for operation with this engine. The cathode shown on the thruster at the top of the photograph in figure 1 is a cold start cathode that was not used during testing.

The thrust produced by the SPT–1 was measured using an inverted pendulum design thrust stand which has been used in previous evaluations of Hall effect thrusters (refs. 11 to 12). Data were taken in a large cryogenically pumped vacuum chamber at NASA GRC. The cylindrical vacuum chamber was 20 m long and 8 m in diameter. During testing the maximum background pressure was 3×10^{-6} torr at a total xenon flow of 5.8 mg/sec. This corresponded to a xenon pumping speed of approximately 250,000 L/sec.

A schematic of the electrical configuration used is shown in figure 2. Commercially available power supplies were used to run the discharge, cathode heater, magnets, and cathode ignitor/keeper. A nonoptimized output filter consisting of a 100 μF capacitor was used between the thruster and the discharge power supply. Independent control of the inner and outer magnet supplies was utilized. This permitted optimization of the magnetic field at each operating point. This was done by systematically adjusting the current to each so as to minimize the discharge current. The effect of this magnet optimization is shown graphically in figure 3. In this case the thruster optimized at approximately 4.5 A of outer magnet current and 7.5 A of inner magnet current. The entire electrical system was allowed to float relative to ground. At no time was the cathode more than 20 V negative with respect to facility ground. This was maintained by using back-to-back 20 V Zener diodes.

The thruster and cathode were operated on commercially available research grade xenon (purity better than 99.9995 percent). A feed system with commercially available mass flow controllers was used to provide the desired flow rates. The flow controllers were calibrated both before and after testing using a constant volume technique. Uncertainties in mass flow rate measurements were estimated to be ±2 percent. The thrust stand was calibrated in-situ using three weights with a mass of approximately 0.010 kg each. The uncertainty in the thrust measurements, primarily due to zero drift, was estimated to be ±1.5 percent. Thrust measurements were taken after operation of the thruster for approximately 1 hr to allow for thruster to approach steady state operating temperatures. At each operating point the inner and outer magnet currents were adjusted to minimize the discharge current at a constant anode flow and discharge voltage. This technique of determining optimal performance by minimizing discharge current has been previously discussed (ref. 13).

RESULTS AND DISCUSSION

The thruster was operated at seven different anode flow rates and voltages ranging from 300 to 1250 V. The maximum voltage tested for a given flow rate corresponded to 3200 W. Operation at powers above 3200 W was not investigated due to thermal limitations of the thruster. The voltage current characteristics from these test data are shown in figure 4. At each point the magnets were adjusted in an attempt to minimize the discharge current. For each anode flow rate the discharge current increases slightly with voltage in a near linear fashion starting at 300 V. At an intermediate voltage, e.g., 750 V for the 2.4 mg/sec anode flow rate case, the discharge current begins to increase at a greater rate with increasing voltage. The increase in discharge current with increasing discharge voltage is near linear above this intermediate voltage as well. The absolute value of the intermediate voltage, where the discharge current versus discharge voltage relationship changed, decreased with increasing anode mass flow rate. The increase in discharge current with increasing discharge voltage for a given anode mass flow rate can be attributable to either an increase in ion current or electron current. It is thought that for 300 V operation the anode propellant is very nearly all singly ionized. Therefore, if the increase in anode current is due to increased ion current, significant number of multiply charged ions must be present. It is also possible that the increase in discharge current at higher voltages was due to electron current. If the increase is due to additional electron current, there must be enhanced axial electron transport across the radial magnetic field region at higher voltages. Additional measurements will need to be made to answer this question definitively.

Figure 5 shows the functional relationship between discharge specific impulse (specific impulse determined based on the anode flow only) and thrust for each of the anode flow rates investigated. For those flow rates that were operated at voltages above 1000 V (2.4 and 2.9 mg/s) a greater than 2:1 spread in both specific impulse and thrust was demonstrated. The lack of high specific impulse points for the higher flow rates was again due to thruster thermal limitations. The rate of increase in discharge specific impulse with thrust is nearly linear in each case, however, as the mass flow rate increases the rate at which the specific impulse increases with thrust is less. This was attributed to an overall increase in discharge efficiency at higher mass flow rates which will be shown in a subsequent figure.

Figure 6 shows the discharge specific impulse plotted versus the discharge voltage. The curve fit is based on the square root of the discharge voltage assuming a simple relationship between the applied voltage and the average exhaust velocity. The curve fit was a best fit to all the data independent of flow rate. The trend at the lower mass flow rates exhibited a slightly lower discharge specific impulse for a given discharge voltage was again attributed to

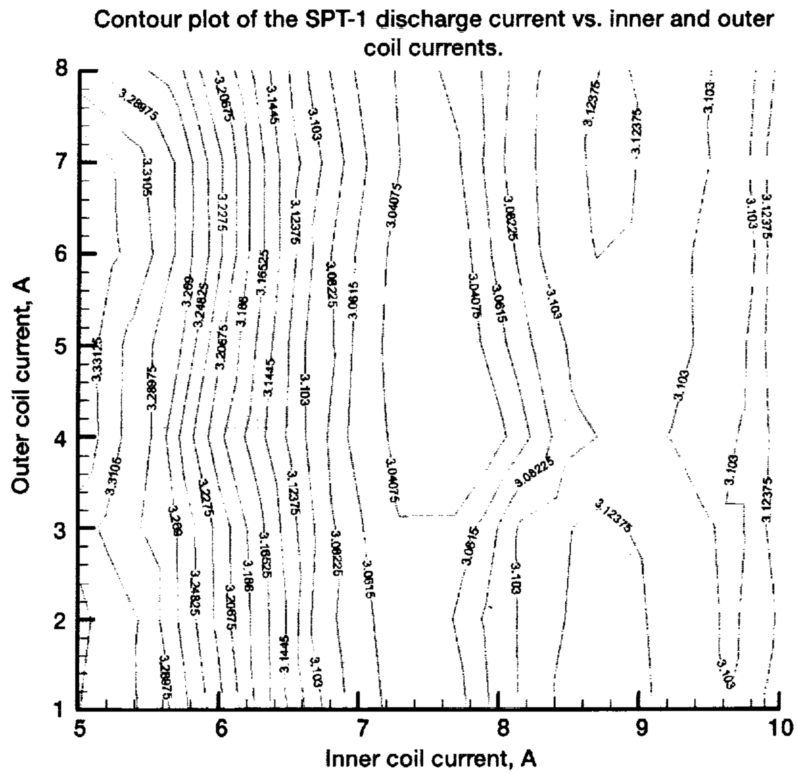

Figure 3.—Effect of magnet current on discharge current.

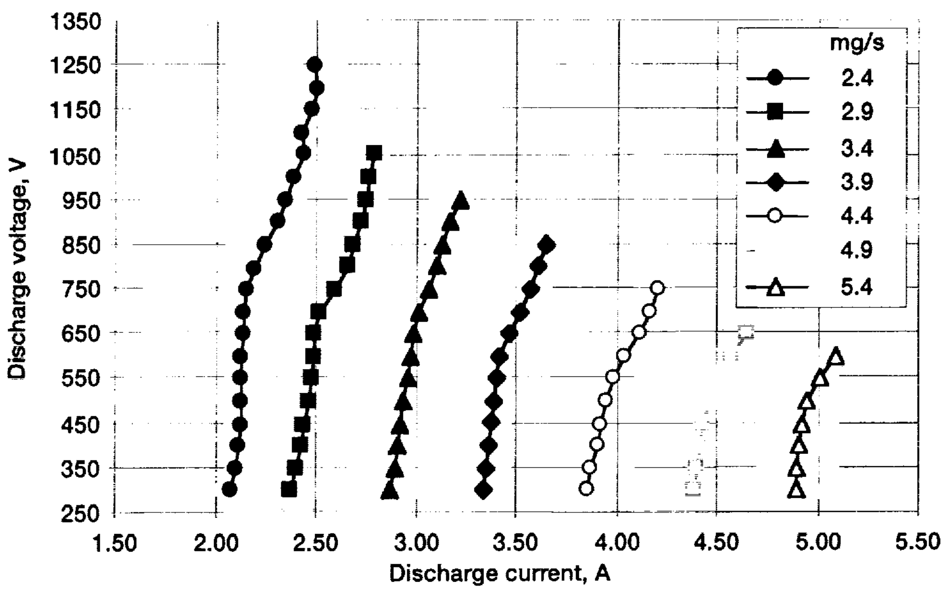

Figure 4.—Voltage/current characteristic.

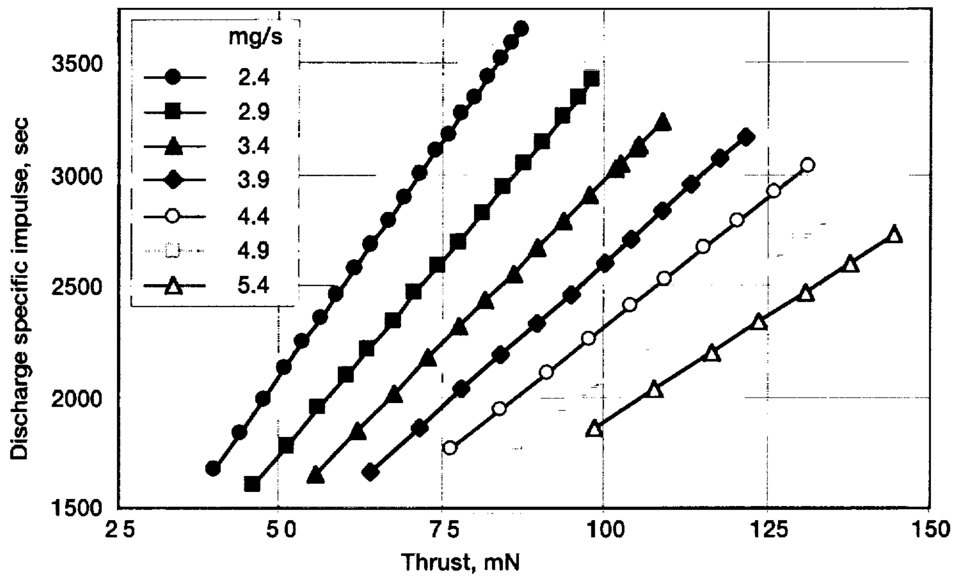

Figure 5.—Discharge specific impulse versus thrust.

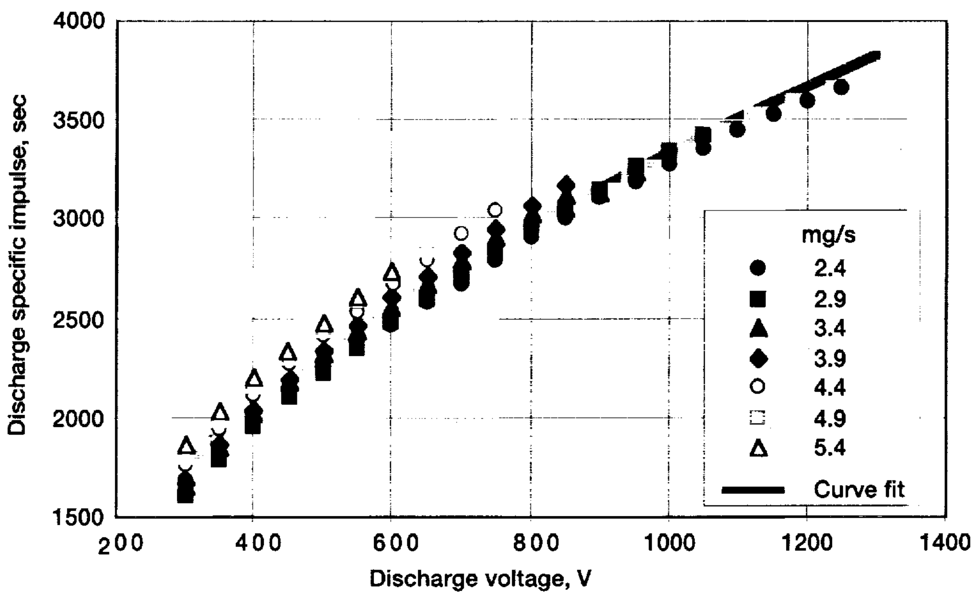

Figure 6.—Discharge specific impulse versus discharge voltage.

an overall increase in discharge efficiency at higher mass flow rates. This also shows that the initial design goal for this engine of 3200 sec of specific impulse was obtained at a discharge voltage near 1000 V.

The suitability of operating the SPT–1 thruster at this high of a voltage is shown in figure 7 where discharge efficiency (efficiency determined based on the anode flow only and discharge power only) is plotted versus discharge voltage. As previously intimated, it can be seen that there was a significant increase in discharge efficiency with increasing anode mass flow rate. It can also be seen that the maximum discharge efficiency for a given anode flow rate occurred at some intermediate discharge voltage. Furthermore, the value of the discharge voltage corresponding to maximum discharge efficiency approximately corresponds to the intermediate voltage mentioned during the discussion of the voltage current characteristics shown in figure 4. Above the optimal discharge voltage the decrease in discharge efficiency is accompanied by an increase in the relative rate of change of discharge current with discharge voltage. This seems to suggest an increase in electron current at elevated voltages rather than multiply charged ions. It is also likely that this relationship between efficiency, voltage, and mass flow rates occurs at channel densities that best optimize the processes of ionization and acceleration with respect to the various thruster loss mechanisms. These data, and similar data obtained by Jacobson et al., (ref. 10) generated using an anode layer thruster do suggest, however, that while ion-thruster-like specific impulses are obtainable with Hall thrusters, efficient operation is obtained at discharge voltages in the 500 to 800 V range which correspond to 2000 to 3000 sec of specific impulse. Based on the variability of the peak efficiency with flow rate and discharge voltage it is clear that a more thorough understanding of these phenomena are needed for optimal design of high voltage stationary plasma thrusters.

To that end the effect of varying the discharge voltage on the optimal magnet settings was considered. In figure 8 the sum of the inner and outer magnet currents are plotted versus discharge voltage. While the sum of the magnet currents is not a precise indicator of the magnetic field strength it is a good indicator of what the radial magnetic field strength is within the channel. It has been suggested that the peak magnetic field strength should scale as the square root of the discharge voltage (ref. 14). In general, these data support this supposition based on the $V^{0.5}$ curve fits shown in the figure. Interestingly, for anode flow rates up to 3.9 mg/s, the curves seem to share the same functional dependency with their slope increasing with anode flow. At anode flow rates of 4.4 mg/s and higher the slope no longer increases with increasing anode flow rate. No clear explanation for this behavior was suggested by the data and it should be reiterated that the sum of the inner and outer magnet currents is only an indicator of the magnetic field strength.

Lastly, the effect of cathode flow rate on high voltage SPT operation was briefly investigated. This was accomplished by varying the cathode flow rate from 0.2 to 1.2 mg/s while the engine was operated at a constant anode flow rate of 3.1 mg/s and a discharge voltage of 800 V. Magnet currents were held constant. The variation in thrust, discharge efficiency, and thruster efficiency versus cathode flow rate are plotted in figure 9. These data show that the cathode flow had a direct effect on thrust. This was thought to be the result of neutral gas from the cathode being ingested into the channel where it is subsequently ionized and accelerated. For cathode flow rates of 0.5 mg/s and above the discharge efficiency remained essentially constant as did the cathode to ground voltage. The lack of change in discharge efficiency with changes in thrust was due to equivalent changes in discharge current which were consistent with the ingestion theory. For cathode flow rates below 0.5 mg/s the discharge efficiency dropped as the cathode-to-ground voltage became more negative. The drop in discharge efficiency could be attributable to a reduction in acceleration voltage since the applied discharge voltage was constant and the cathode-to-ground voltage became more negative. This assumes the plasma beam exiting the thruster is close to facility ground. At these lower cathode flow rates the overall thruster efficiency reached a maximum of 46 percent. Additional tests were not conducted to determine the optimal cathode flow rate at other operating conditions. The cathode flow rate for all the previously reported data was 0.4 mg/s.

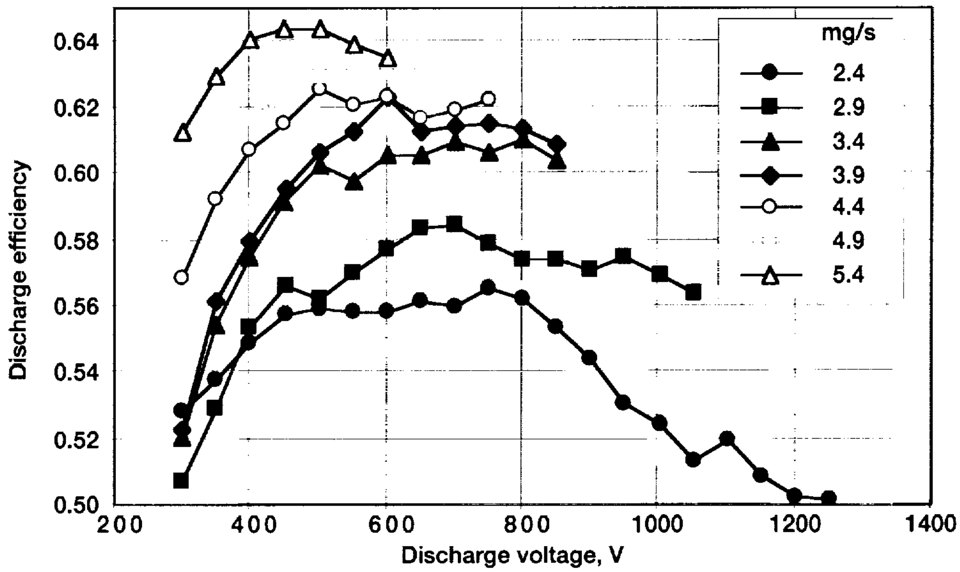

Figure 7.—Discharge efficiency versus discharge voltage.

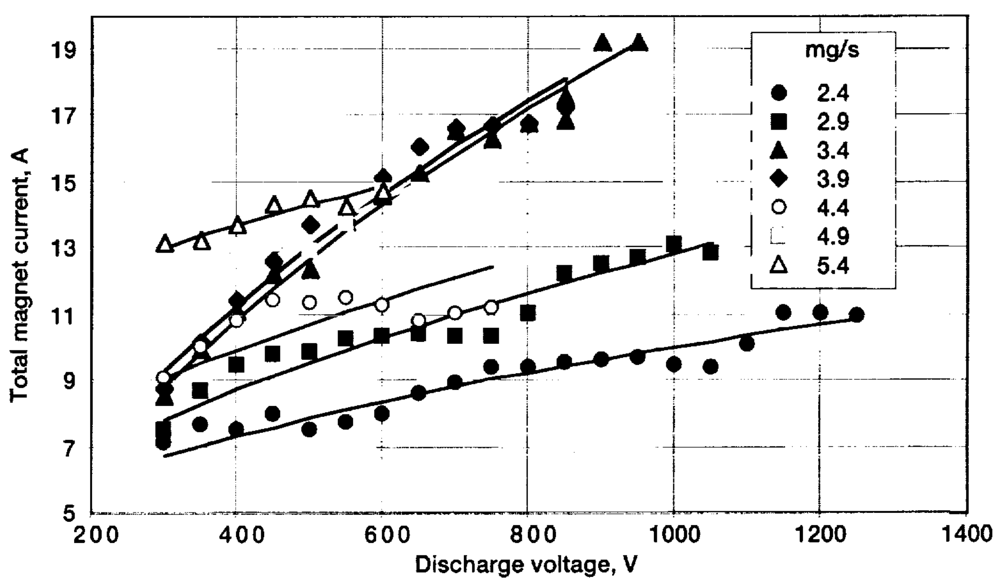

Figure 8.—Total magnet current versus discharge voltage.

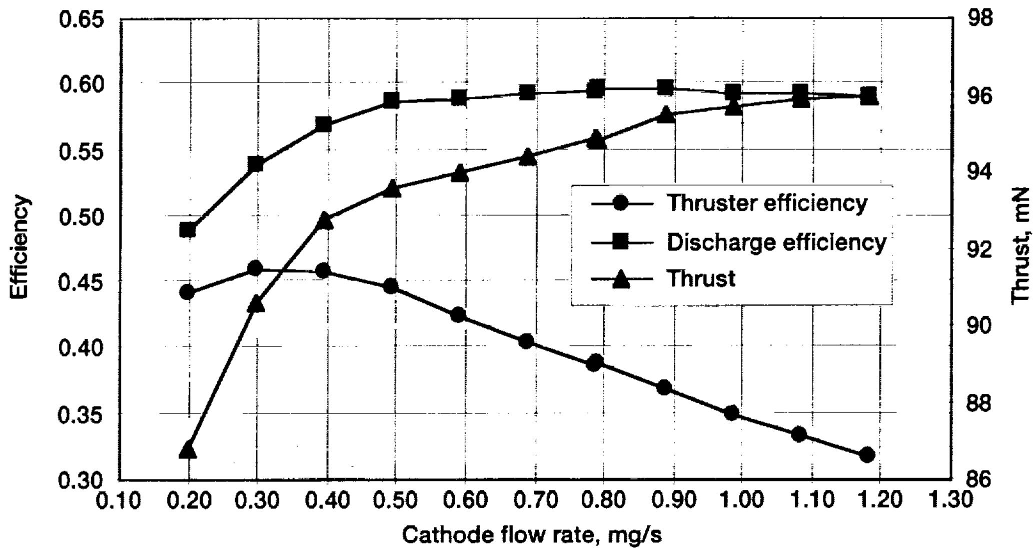

Figure 9.—Discharge efficiency, thruster efficiency, and thrust versus cathode flow rate.

CONCLUSIONS

Operation of the SPT–1 high voltage stationary plasma thruster demonstrated that it is possible to expand the operational envelope of Hall thrusters from the 300 V, 1500 sec specific impulse range to voltages in excess of 1000 V and specific impulses approaching that of state-of-the-art gridded ion thrusters. Discharge specific impulses in excess of 3500 sec were measured at discharge voltages above 1200 V. For a given anode mass flow rate that did not result in thermal limitations the thruster could roughly be throttled over a 2:1 range in both thrust and therefore specific impulse. These data also demonstrated that discharge specific impulse is primarily dependant on discharge voltage, with a secondary anode mass flow rate effect due to more efficient operation at increased anode mass flow rates.

The performance data taken during this investigation indicated that discharge voltage can be optimized for maximum discharge efficiency. Generally this optimal discharge voltage was in the 500 to 700 V range although the optimal value varied with anode flow rate. These data in conjunction with measured voltage current characteristics suggest that there is a loss mechanism at high voltages that results in a higher than anticipated discharge current for a given anode flow rate. A possible cause of this is increased electron transport across the magnetic field region. Additional tests would be needed to verify this theory. The variation in optimum magnetic field strength with discharge voltage was shown to follow a $V^{0.5}$ dependence as expected. Finally the effect of cathode flow fraction on thruster efficiency was investigated while operating with an 800 V discharge voltage. These data show there is an optimal cathode flow rate with respect to thruster efficiency that does not necessarily correspond with maximum thrust or discharge efficiency.

APPENDIX

Discharge voltage, V	Discharge current, A	Discharge power, W	Anode flow, mg/s	Cathode flow, mg/s	V mag inner, V	I mag inner, A	V mag outer, V	I mag outer, A	Magnet power, W	Total power, W	Thrust, mN	Isp, sec	Isp*	Eff	Eff*	Cathode ground, V
300	2.07	621	2.42	0.43	2.59	4.06	3.25	3.05	20.4	642	39.9	1424	1679	0.39	0.53	−14.8
350	2.10	736	2.42	0.43	2.68	4.21	3.35	3.44	22.8	758	43.8	1563	1843	0.40	0,54	−14.4
401	2.11	845	2.42	0.43	2.7	4.34	3.37	3.17	22.4	868	47.4	1692	1994	0.41	0.55	−14.3
451	2.12	955	2.42	0.43	2.83	4.58	3.54	3.44	25.1	980	50.8	1813	2138	0.42	0.56	−14.3
500	2.12	1061	2.42	0.43	2.58	4.18	3.21	3.35	21.5	1082	53.6	1913	2255	0.42	0.56	−13.8
550	2.12	1167	2.42	0.43	2.6	4.21	3.22	3.55	22.4	1189	56.2	2006	2365	0.42	0.56	−13.6
600	2.12	1273	2.42	0.43	2.64	4.3	3.27	3.67	23.4	1296	58.7	2095	2470	0.42	0.56	−13.6
650	2.13	1385	2.42	0.43	2.75	4.5	3.4	4.12	26.4	1411	61.4	2191	2584	0.42	0.56	−13.7
701	2.14	1500	2.42	0.43	2.84	4.65	3.51	4.28	28.2	1528	63.8	2277	2685	0.42	0.56	−14.3
750	2.15	1613	2.42	0.43	2.94	4.79	3.62	4.59	30.7	1644	66.5	2373	2798	0.42	0.57	−14.5
800	2.19	1752	2.42	0.43	2.94	4.79	3.63	4.59	30.7	1783	69.1	2466	2908	0.42	0.56	−14.3
850	2.24	1905	2.42	0.43	3.06	5.01	3.8	4.51	32.5	1937	71.5	2552	3009	0.42	0.55	−14.2
900	2.30	2071	2.42	0.43	3.17	5.2	3.95	4.41	33.9	2105	73.9	2637	3110	0.41	0.54	−14.2
951	2.35	2234	2.42	0.43	3.2	5.21	4.01	4.47	34.6	2269	75.8	2705	3189	0.40	0.53	−14.5
1001	2.38	2382	2.42	0.43	3.28	5.36	4.13	4.12	34.6	2416	77.8	2777	3274	0.39	0.52	−14.3
1051	2.43	2553	2.42	0.43	3.25	5.29	4.12	4.09	34.0	2587	79.7	2844	3354	0.39	0.51	−14.5
1100	2.42	2663	2.42	0.43	3.61	5.83	4.61	4.29	40.8	2704	81.9	2923	3446	0.39	0.52	−14.3
1151	2.48	2854	2.42	0.43	3.98	6.34	5.1	4.67	49.1	2903	83.9	2994	3530	0.38	0.51	−14.4
1200	2.50	3001	2.42	0.43	4.02	6.34	5.18	4.67	49.7	3051	85.5	3051	3598	0.38	0.50	−14.7
1251	2.49	3114	2.42	0.43	4.06	6.33	5.25	4.67	50.2	3164	87	3105	3661	0.38	0.50	−14.8
300	2.37	713	2.92	0.43	2.804	4.098	3.566	3.39	23.6	736	45.92	1398	1605	0.39	0.51	−17.7
350	2.40	841	2.92	0.43	3.13	4.647	3.957	4.019	30.4	871	50.96	1551	1782	0.41	0.53	−17.9
400	2.42	970	2.92	0.43	3.305	4.934	4.161	4.561	35.3	1006	55.98	1704	1957	0.43	0.55	−17.9
451	2.44	1099	2.92	0.43	3.447	5.226	4.331	4.551	37.7	1136	60.234	1833	2106	0.44	0.57	−18.0
501	2.46	1232	2.92	0.43	3.521	5.402	4.418	4.496	38.9	1271	63.57	1935	2223	0.43	0.56	−17.8
550	2.48	1362	2.92	0.43	3.641	5.625	4.564	4.615	41.5	1404	67.29	2048	2353	0.44	0.57	−17.7
600	2.48	1490	2.92	0.43	3.734	5.825	4.68	4.529	42.9	1533	70.84	2156	2477	0.45	0.58	−17.7
650	2.49	1619	2.92	0.43	3.82	6.024	4.785	4.377	44.0	1663	74.24	2259	2596	0.45	0.58	−17.8
700	2.51	1755	2.92	0.43	3.754	5.914	4.699	4.443	43.1	1798	77.37	2355	2705	0.45	0.58	−17.6
751	2.59	1945	2.92	0.43	3.698	5.826	4.625	4.487	42.3	1987	81.01	2466	2832	0.45	0.58	−16.8
801	2.65	2124	2.92	0.43	4.156	6.606	5.214	4.466	50.7	2175	84.35	2567	2949	0.45	0.57	−16.7
851	2.68	2282	2.92	0.43	4.803	7.634	6.046	4.606	64.5	2347	87.408	2660	3056	0.44	0.57	−16.7
900	2.72	2446	2.92	0.43	4.982	7.842	6.282	4.681	68.5	2514	90.224	2746	3154	0.44	0.57	−16.7
951	2.75	2612	2.92	0.43	5.15	8.056	6.508	4.629	71.6	2684	93.58	2848	3272	0.45	0.57	−16.4
1001	2.76	2764	2.92	0.43	5.388	8.329	6.824	4.781	77.5	2842	95.78	2915	3349	0.44	0.57	−16.3
1050	2.78	2922	2.92	0.43	5.46	8.362	6.939	4.525	77.1	2999	98.03	2984	3427	0.44	0.56	−16.2
301	2.87	861	3.41	0.43	2.265	4.011	2.832	4.511	21.9	883	55.27	1466	1653	0.42	0.52	−17.3
350	2.89	1011	3.41	0.43	2.971	5.233	2.914	4.68	29.2	1041	61.81	1640	1848	0.44	0.55	−17.5
400	2.91	1164	3.41	0.43	3.498	6.131	3.108	4.994	37.0	1201	67.56	1792	2020	0.46	0.58	−17.5
450	2.92	1314	3.41	0.43	3.992	6.937	3.313	5.307	45.3	1359	72.81	1932	2177	0.47	0.59	−17.6
500	2.93	1466	3.41	0.43	4.164	7.166	3.281	5.23	47.0	1513	77.612	2059	2321	0.48	0.60	−17.4
551	2.96	1631	3.41	0.43	4.928	8.314	3.442	5.468	59.8	1690	81.52	2163	2438	0.47	0.60	−17.1
600	2.97	1782	3.41	0.43	5.367	8.892	3.584	5.65	68.0	1850	85.784	2276	2565	0.48	0.61	−17.0
651	2.98	1941	3.41	0.43	5.784	9.399	3.797	5.922	76.8	2018	89.56	2376	2678	0.48	0.61	−17.0
700	3.01	2108	3.41	0.43	6.777	10.6	3.851	5.962	94.8	2203	93.61	2483	2799	0.48	0.61	−16.9
750	3.05	2291	3.41	0.43	6.797	10.35	3.891	5.918	93.4	2384	97.36	2583	2912	0.48	0.61	−16.6
800	3.09	2476	3.41	0.43	7.338	10.87	3.939	5.917	103.1	2579	101.51	2693	3036	0.48	0.61	−16.3

Discharge voltage, V	Discharge current, A	Discharge power, W	Anode flow, mg/s	Cathode flow, mg/s	V mag inner, V	I mag inner, A	V mag outer, V	I mag outer, A	Magnet power, W	Total power, W	Thrust, mN	Isp, sec	Isp*	Eff	Eff*	Cathode ground, V
850	3.13	2659	3.41	0.43	7.843	11.37	3.668	5.473	109.2	2768	104.63	2776	3129	0.48	0.60	−15.8
851	3.13	2660	3.41	0.43	7.334	11.54	9.277	6.056	140.8	2801	102.15	2710	3055	0.45	0.58	−19.1
900	3.17	2852	3.41	0.43	8.641	12.88	11.036	6.326	181.1	3033	104.98	2785	3140	0.44	0.57	−19.5
951	3.22	3061	3.41	0.43	9.044	13.03	11.621	6.207	189.9	3251	108.54	2880	3246	0.44	0.56	−19.4
300	3.33	1000	3.90	0.43	2.4	4.3	2.87	4.49	23.2	1023	63.87	1502	1669	0.43	0.52	−16.9
351	3.34	1171	3.90	0.43	3.26	5.77	2.8	4.42	31.2	1202	71.61	1684	1871	0.46	0.56	−16.9
401	3.36	1346	3.90	0.43	3.71	6.53	3.11	4.89	39.4	1385	78.02	1834	2038	0.47	0.58	−17.1
451	3.37	1519	3.90	0.43	4.24	7.37	3.35	5.26	48.9	1568	84.04	1976	2196	0.49	0.60	−17.1
501	3.38	1692	3.90	0.43	4.763	8.141	3.609	5.606	59.0	1751	89.47	2104	2338	0.49	0.61	−17.2
551	3.40	1870	3.90	0.43	4.816	8.137	3.668	5.65	59.9	1929	94.56	2223	2471	0.50	0.61	−17.2
600	3.41	2046	3.90	0.43	5.801	9.532	3.643	5.606	75.7	2122	99.76	2346	2606	0.51	0.62	−16.9
650	3.46	2251	3.90	0.43	6.42	10.3	3.791	5.79	88.1	2339	103.76	2440	2711	0.50	0.61	−16.6
700	3.51	2461	3.90	0.43	6.756	10.58	4.024	6.074	95.9	2557	108.6	2554	2837	0.50	0.61	−16.6
750	3.56	2673	3.90	0.43	6.976	10.68	4.005	5.985	98.5	2772	113.27	2663	2959	0.50	0.61	−17.3
801	3.61	2890	3.90	0.43	7.296	10.94	3.935	5.843	102.8	2993	117.69	2767	3075	0.50	0.61	−15.9
850	3.65	3102	3.90	0.43	8.022	11.69	3.75	5.561	114.6	3217	121.43	2855	3173	0.49	0.61	−15.46
301	3.85	1158	4.39	0.43	2.57	4.57	3.1	4.5	25.7	1184	76.1	1607	1765	0.48	0.57	−15.5
350	3.87	1356	4.39	0.43	2.91	5.16	3.52	4.9	32.3	1388	84	1773	1948	0.50	0.59	−16.2
401	3.90	1562	4.39	0.43	3.15	5.55	3.83	5.27	37.7	1600	91.3	1928	2118	0.51	0.61	−16.3
450	3.92	1765	4.39	0.43	3.35	5.82	4.09	5.64	42.6	1807	97.7	2063	2266	0.51	0.62	−16.2
500	3.94	1972	4.39	0.43	3.33	5.71	4.08	5.62	41.9	2014	104.1	2198	2415	0.52	0.63	−15.9
550	3.98	2190	4.39	0.43	3.32	5.63	4.08	5.86	42.6	2233	109.3	2308	2535	0.52	0.62	−14.7
601	4.03	2422	4.39	0.43	3.43	5.85	4.24	5.41	43.0	2465	115.2	2432	2672	0.52	0.62	−14.2
650	4.11	2672	4.39	0.43	3.24	5.43	4.01	5.41	39.3	2712	120.4	2542	2793	0.52	0.62	−13.8
700	4.16	2912	4.39	0.43	3.28	5.45	4.07	5.58	40.6	2953	125.9	2658	2920	0.52	0.62	−14.3
750	4.20	3151	4.39	0.43	3.36	5.55	4.18	5.67	42.3	3194	131.3	2772	3046	0.53	0.62	−14.4
300	4.38	1316	4.89	0.43	3.06	4.85	3.79	6.1	38.0	1354	86.3	1653	1800	0.49	0.58	−15.7
350	4.39	1537	4.89	0.43	3.32	5.27	4.1	6.34	43.5	1581	95.2	1824	1986	0.51	0.60	−15.9
400	4.41	1766	4.89	0.43	3.62	5.68	4.47	7.21	52.8	1819	103.2	1977	2152	0.52	0.62	−16.0
451	4.42	1992	4.89	0.43	3.79	5.95	4.69	7.23	56.5	2049	110.4	2115	2303	0.53	0.63	−15.9
500	4.46	2232	4.89	0.43	3.71	5.81	4.6	7.09	54.2	2286	117.2	2245	2444	0.53	0.63	−15.5
551	4.51	2483	4.89	0.43	3.92	6.06	4.86	7.63	60.8	2544	123.8	2372	2582	0.54	0.63	−14.5
601	4.57	2744	4.89	0.43	4.44	6.89	5.53	7.82	73.8	2818	130	2490	2711	0.53	0.63	−14.7
651	4.64	3018	4.89	0.43	4.44	6.77	5.53	7.97	74.1	3092	136.4	2613	2845	0.54	0.63	−14.3
300	4.89	1468	5.38	0.43	3.52	5.07	4.35	8.1	53.1	1522	98.4	1725	1864	0.52	0.61	−11.9
350	4.89	1713	5.38	0.43	3.79	5.61	4.69	7.64	57.1	1770	107.7	1888	2040	0.54	0.63	−12.3
400	4.90	1960	5.38	0.43	4	5.97	4.97	7.73	62.3	2022	116.2	2037	2201	0.55	0.64	−12.5
450	4.91	2210	5.38	0.43	4.16	6.16	5.16	8.15	67.7	2278	123.7	2169	2344	0.55	0.64	−12.4
500	4.94	2471	5.38	0.43	4.22	6.24	5.24	8.26	69.6	2541	130.8	2293	2478	0.55	0.64	−12.4
550	5.01	2757	5.38	0.43	4.17	6.14	5.18	8.09	67.5	2825	137.7	2414	2609	0.55	0.64	−12.2
600	5.09	3056	5.38	0.43	4.29	6.25	5.32	8.52	72.1	3128	144.5	2533	2738	0.55	0.63	−12.0

REFERENCES

1. Day, M., et. al.: "Stationary Plasma Thruster-100 Subsystem Qualification Status," AIAA-96–2713, July 1996.
2. Hargus, W., Fife, M., McFall, K., Jankovsky, R., and Mason, L.: "Status of U.S. Testing of the High Performance Hall System SPT-140 Hall Thruster," AIAA-2000–1053, January 2000.
3. Lynn, P., Osborn, M., Sankovic, J., and Caveny, L.: "Electric Propulsion Demonstration Module (EPDM) Flight Hall Thruster System," IEPC-97–100, August 1997.
4. Oleson, S. and Myers, R.: "Advanced Propulsion for Geostationary Orbit Insertion and North-South Station Keeping," AIAA-95–2513, July 1995.
5. Oleson, S.: "Electric Propulsion for Low Earth Orbit Communication Satellites," IEPC-97–148, August 1997.
6. Spanjers, G., Birjan, M., and Lawrence, T.: "The USAF Electric Propulsion Research Program," AIAA-2000–3146, July 2000.
7. Oleson, S.: "Advanced Propulsion for Space Solar Power Satellites," AIAA-99–2872, June 1999.
8. Gefert, L., Hack, J., and Kerslake, T.: "Options for the Human Exploration of Mars Using Solar Electric Power," *Proceedings of the Space Technology and Applications International Forum–1999.*
9. Oleson, S.: "Mission Advantages of Constant Power Variable Isp Electrostatic Thrusters," AIAA-2000–3413, July 2000.
10. Jacobson, D., Jankovsky, R., and Manzella, D.: "High Voltage TAL Performance," AIAA-2001–3777, July 2001.
11. Sankovic, J.M., Haag, T.W., and Manzella, D.H.: "Operating Characteristics of the Russian D-55 Thruster with Anode Layer," AIAA-94–3011, June 1994.
12. Sankovic, J.M., Haag, T.W., and Manzella, D.H.: "Performance Evaluation of a 4.5 kW SPT Thruster," IEPC-95–30, Sept. 1995.
13. Gavryushin, V., et. al.: "Study of the Effect of Magnetic Field Variations, Channel Geometry and its Wall Contamination Upon the SPT Performance," AIAA-94–2854, June 1994.
14. Belan, N., et. al.: *Statsionarnyye Plasmennyye Dvigateli*, USSR State Committee on Public Education, N. Yr. Zhukovskiy Kharkov Order of Lenin Institute, Kharkov, 1989.

REPORT DOCUMENTATION PAGE

Form Approved
OMB No. 0704-0188

1. AGENCY USE ONLY (*Leave blank*)	2. REPORT DATE	3. REPORT TYPE AND DATES COVERED
	November 2001	Technical Memorandum

4. TITLE AND SUBTITLE

High Voltage SPT Performance

5. FUNDING NUMBERS

WU–755–B4–05–00

6. AUTHOR(S)

David Manzella, David Jacobson, and Robert Jankovsky

7. PERFORMING ORGANIZATION NAME(S) AND ADDRESS(ES)

National Aeronautics and Space Administration
John H. Glenn Research Center at Lewis Field
Cleveland, Ohio 44135–3191

8. PERFORMING ORGANIZATION REPORT NUMBER

E–12983

9. SPONSORING/MONITORING AGENCY NAME(S) AND ADDRESS(ES)

National Aeronautics and Space Administration
Washington, DC 20546–0001

10. SPONSORING/MONITORING AGENCY REPORT NUMBER

NASA TM—2001-211135
AIAA–2001–3774

11. SUPPLEMENTARY NOTES

Prepared for the 37th Joint Propulsion Conference and Exhibit cosponsored by the AIAA, SAE, AIChE, and ASME, Salt Lake City, Utah, July 8–11, 2001. David Manzella, University of Toledo, 2801 W. Bancroft Street, Toledo, Ohio 43606–3328; David Jacobson and Robert Jankovsky, NASA Glenn Research Center. Responsible person, David Manzella, organization code 5430, 216–977–7432.

12a. DISTRIBUTION/AVAILABILITY STATEMENT

Unclassified - Unlimited
Subject Category: 20 Distribution: Nonstandard

Available electronically at http://gltrs.grc.nasa.gov/GLTRS

This publication is available from the NASA Center for AeroSpace Information, 301–621–0390.

12b. DISTRIBUTION CODE

13. ABSTRACT *(Maximum 200 words)*

A 2.3 kW stationary plasma thruster designed to operate at high voltage was tested at discharge voltages between 300 and 1250 V. Discharge specific impulses between 1600 and 3700 sec were demonstrated with thrust between 40 and 145 mN. Test data indicated that discharge voltage can be optimized for maximum discharge efficiency. The optimum discharge voltage was between 500 and 700 V for the various anode mass flow rates considered. The effect of operating voltage on optimal magnet field strength was investigated. The effect of cathode flow rate on thruster efficiency was considered for an 800 V discharge.

14. SUBJECT TERMS

Electric propulsion

15. NUMBER OF PAGES

17

16. PRICE CODE

17. SECURITY CLASSIFICATION OF REPORT	18. SECURITY CLASSIFICATION OF THIS PAGE	19. SECURITY CLASSIFICATION OF ABSTRACT	20. LIMITATION OF ABSTRACT
Unclassified	Unclassified	Unclassified	

NSN 7540-01-280-5500

Standard Form 298 (Rev. 2-89)
Prescribed by ANSI Std. Z39-18
298-102